On the impact of rainfall patterns on the hydrologic response

L. Nicótina,[1] E. Alessi Celegon,[1] A. Rinaldo,[1,2] and M. Marani[1]

Received 13 November 2007; revised 1 August 2008; accepted 26 August 2008; published 2 December 2008.

[1] We study the influence exerted by space-time rainfall patterns on the hydrologic response to determine the scales for which the spatial heterogeneity of rainfall may play a significant role in shaping the hydrographs generated in basins of varying characteristics. We perform numerical experiments using models based on the geomorphological theory of the hydrologic response, in which the spatial resolution of the input rainfall fields is coarse grained from 100 m to 50 km. The variation in the resulting hydrographs shows that rainfall spatial variability does not significantly influence the flood response for basin areas up to about 3500 km^2 in the cases considered, provided that the rainfall volume at each time interval is preserved. We then search for the physical interpretation of these results using the Jensen-Shannon divergence measure to characterize differences in travel time distributions sampled by real and idealized disk-shaped rainfall patterns of different size. Because the total residence time of a water parcel is often controlled by the travel time within hillslopes, we find that when typical hillslope size is smaller than the characteristic size of rainfall structures (say, a correlation length of rainfall intensity), the rainfall pattern effectively samples all possible residence times and the response of the catchment does not depend on the specific rainfall pattern. In larger basins (say, typically larger than 10^3 km^2) the travel time in the channels is expected to be an important part of the total residence time. In this case the response of a catchment will also be controlled by the specifics of the spatial distribution of rainfall.

Citation: Nicótina, L., E. Alessi Celegon, A. Rinaldo, and M. Marani (2008), On the impact of rainfall patterns on the hydrologic response, *Water Resour. Res.*, *44*, W12401, doi:10.1029/2007WR006654.

1. Introduction

[2] Rainfall is a highly heterogeneous process over a wide range of scales both in space and time [e.g., *Lovejoy and Schertzer*, 1985; *Rodriguez-Iturbe et al.*, 1998; *Marani*, 2005]. As a result, the determination of the detail required to capture the relevant heterogeneities and to accurately describe the components of the hydrologic cycle, e.g., for hydrologic/climate modeling, is a very important open problem [e.g., *Eagleson*, 1978; *Salvucci and Entekhabi*, 1995; *Marani et al.*, 1997]. In particular, answers to this important research question have not been unequivocal, and conflicting conclusions have been put forward in the literature. *Wilson et al.* [1979] evaluated the response of a small natural catchment using a deterministic modeling framework based on the kinematic wave approximation and explored different space-time distributions of synthetic rainfall fields. Their conclusions call for a detailed space-time representation of rainfall in distributed hydrologic models. However, they do not discuss the physical mechanisms responsible for the suggested influence of rainfall distribution on the hydrologic response, nor do they consider the possible effect of catchment scale. On the other hand, *Krajewski et al.* [1991], with an experimental setup comparable to that of *Wilson et al.* [1979], conclude that rainfall temporal variability, rather than its spatial distribution, plays a primary role in the hydrologic response. *Krajewski et al.* [1991] examine the hydrologic response in terms of peak discharge and time to peak for a very small catchment (7.5 km^2) and do not find significant relationships between spatial rainfall heterogeneity and runoff response. Surface hydrologic partitioning processes are indicated as one of the main sources of variability in catchment response by *Shah et al.* [1996]. On the basis of a physically based distributed hydrologic model applied to a small (10.55 km^2) upland catchment, they relate the role of rainfall heterogeneities to antecedent catchment conditions, finding a significant change in runoff response only for low initial water content. These findings are also supported by *Segond et al.* [2007], who, on the basis of numerical experiments in a midsized catchment (1400 km^2), identify runoff production mechanisms as the dominant source of variability in runoff response. They also suggest that the effect of rainfall spatial variability is damped by catchment dimension, while the sensitivity to spatial rainfall is obviously increased by increased runoff production (say, by urbanization). Quite to the contrary, *Smith et al.* [2005] observe that spatial rainfall variability does not significantly influence the hydrologic response in a fully urban catchment (14.3 km^2). They report that even highly spatially

[1]Dipartimento di Ingegneria Idraulica, Marittima, Ambientale e Geotecnica and International Center for Hydrology "Dino Tonini," Universitá di Padova, Padua, Italy.

[2]Laboratory of Ecohydrology ECHO/ISTE/ENAC/EPFL, Ecole Polytechnique Fédérale, Lausanne, Switzerland.

0043-1397/08/2007WR006654

Figure 1. Geographic location of the study catchments.

variable rainfall fields did not produce significant changes in the observed discharge because of the "mixing" effect operated by the drainage network: rainfall spatial variability is much lower in a non-Euclidean space defined along the drainage network structure. A different perspective to the problem is presented by *Gabellani et al.* [2007], whose experiments, carried out on catchments of different sizes, show significant changes (up to 25% in peak discharge) in the hydrologic response for storm events with different space-time structures. They also suggest that the importance of rainfall heterogeneity depends on the ratio of the characteristic spatial scale of rainfall and catchment size emphasized by the nonlinearities of the runoff production.

[3] In summary, although most of the previous works refer to relatively small catchments (with areas smaller than 10^2 km^2, i.e., smaller or comparable to mesoscale rainfall structures [*Winchell et al.*, 1998; *Dodov and Foufoula-Georgiou*, 2005]), the literature addressing the role of rainfall spatial variability includes quite heterogeneous approaches in terms of the tools adopted, studied catchments, and conclusions drawn from the analyses. Some hypotheses have been put forward to identify the mechanisms through which rainfall spatial variability may affect catchment response, with an emphasis on hydrologic partitioning processes [e.g., *Shah et al.*, 1996; *Brath and Montanari*, 2003; *Gabellani et al.*, 2007], whereas the effects of transport processes along the channel network have usually not been considered. To the best of our knowledge, no attempts have been made to relate the spatial scales of heterogeneity of rainfall and the heterogeneities embedded in the basin geomorphic structure (with the exception of *Smith et al.* [2005], who deal, however, with a very small urban catchment). Thus, we believe there is a need to clarify the extent of the possible influence of rainfall spatial variability on the hydrologic response, as a function of basin scale, characteristic spatial scales of rainfall events, runoff generation mechanisms, and water transport processes in hillslopes and the channel network.

[4] Here we seek to determine, through careful numerical experiments, the spatial scales at which rainfall variability may be expected to play a relevant role in shaping the main features of hydrographs in basins of varying characteristics. An important issue is related to the effects of rainfall spatial distribution as a function of catchment area. In particular, the effects of the spatial di ion of rainfall are generally expected to become important for increasing catchment area. In order to clarify this possible dependence we use extensively validated geomorphological models of the hydrologic response applied to a wide variety of basins in temperate climates with areas in the range $O(10^2–10^3)$ km^2 (Figure 1). We perform numerical experiments in which the spatial resolution of the input rainfall fields is coarse grained from 100 m to 50 km to explore the influence of the representation of rainfall variability on hydrograph characteristics.

[5] Effects of spatial rainfall variability on flood hydrographs may be induced by heterogeneous paths sampled by different rainfall distributions as well as by marked spatial heterogeneities in runoff generation. In order to separately address these effects we perform numerical experiments in which infiltration is "turned off" by assuming that the soil is perfectly impermeable throughout the basin. We then interpret the physical mechanisms giving rise to the obtained results in terms of the conditional travel time distributions sampled by rainfall structures from the overall travel time distribution of the basin represented by its width function [e.g., *Rodriguez-Iturbe and Rinaldo*, 1997; *Lashermes and Foufoula-Georgiou*, 2007] using tools derived from information theory [*Lin*, 1991; *Grosse et al.*, 2002]. The conclusions drawn from our numerical studies are reinforced by the physical foundation of the models used, based on water travel time distributions, and by their ability to accurately and robustly represent the hydrologic response of several different systems subject to rainfall events characterized by widely different space-time structures.

2. Methods

[6] The hydrological model relies on a fully distributed processing of the rainfall forcing [see also *Rinaldo et al.*, 2006a, 2006b], which is assigned on a 100 m × 100 m grid (e.g., see Figure 2) through ordinary kriging of rain gauge observations using experimental variograms [e.g., *Goovaerts*, 1997] (e.g., see *Lebel et al.* [1987] for a discussion on the appropriateness of kriging for rainfall estimation, and see section 3 for details on the observation network in the basins considered).

[7] Runoff computations, applied at the subcatchment scale (see below for details on subcatchment extraction

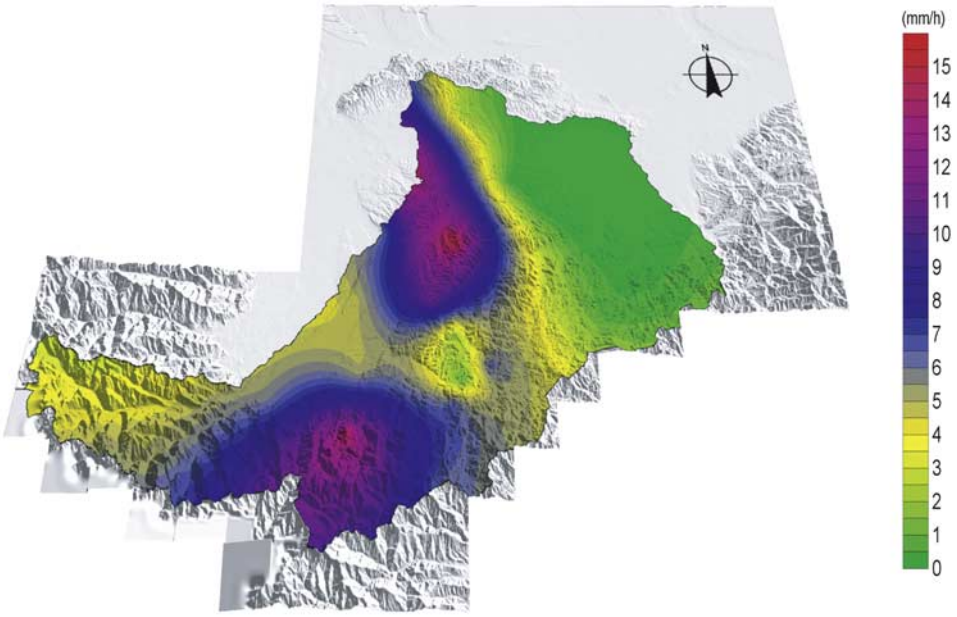

Figure 2. Interpolated hourly rainfall field for the Tanaro catchment during the November 1994 event.

and characteristics), are performed using a Green-Ampt scheme for shallow soils (depth of the soil layer ΔZ) with unsteady rain [*Green and Ampt*, 1911; *Chu*, 1978; *Dingman*, 1994; *Barry et al.*, 2005]. Briefly, the infiltration rate ($j(t)$) is represented as a function of cumulative infiltration ($I(t)$) and of the vertically homogeneous soil properties:

$$j(t) = K_{\text{sat}}\left[1 + \frac{|\psi_f|(\Phi - \theta_0)}{I(t)}\right], \tag{1}$$

where K_{sat} is the hydraulic conductivity of the soil at saturation, ψ_f is the effective pressure head at the wetting front, Φ is the porosity of the soil layer, and θ_0 is the initial water content. Whenever rainfall intensity exceeds the infiltration rate, (Hortonian) infiltration excess runoff occurs. After ponding (at t_p), a sharp wetting front propagates downward at a rate $j(t)/(\phi - \theta_0)$ and may (if the duration of the event is large enough) eventually reach the bottom of the interacting soil layer (at depth ΔZ [e.g., *Dingman*, 1994]); at this time, saturation excess runoff starts to occur. The adopted formulation of the Green and Ampt model has been chosen because it provides a simple (but not simplistic [e.g., *Barry et al.*, 2005]) and yet physically based description of both infiltration excess and saturation excess mechanisms, which is crucial for a realistic representation of actual runoff generation processes. Note that exercises with different runoff formation models, not reported for brevity, have been reported elsewhere [*Rinaldo et al.*, 2002; *Settin et al.*, 2005].

[8] A prescribed fraction of the infiltrating volume contributes to the recharge of the water table (deep percolation), while the residual fraction, say η, contributes to the (shallow) subsurface flow toward the channel network. Because the interest is here on the flood response of the system, deep percolation is not routed to the outlet as it is not expected to contribute at the event timescale.

[9] Water routing of the surface and subsurface components is performed by defining the corresponding geomorphologic unit hydrograph (GIUH) [*Rinaldo and Rodriguez-Iturbe*, 1996]. The GIUH of each component is, by definition, the probability density function (pdf), $f(t)$, of the travel time of water parcels within the basin. The travel time distribution at the basin outlet is obtained by evaluating the residence time distributions over the set of all the possible (surface or subsurface) paths (Γ) leading to the outlet [*Rodriguez-Iturbe and Rinaldo*, 1997]:

$$f(t) = \sum_{\gamma \in \Gamma} p(\gamma, t) f_{h_\gamma} * f_{c_m} * f_{c_{m+1}} * \ \ldots * f_{c_n}(t), \tag{2}$$

where the asterisk is the convolution operator, $p(\gamma, t)$ is the probability that a water parcel follows path $\gamma \in \Gamma$, and $f_{h_\gamma}(t)$ is the pdf of residence times within the source hillslope (h_γ) where the path γ is originated. This pdf is assumed to be exponential with mean residence time $\overline{t}_{\gamma,k} = \lambda_k \times A_\gamma^{0.38}$, where A_γ is the area of hillslope h_γ [*Boyd*, 1978; *D'Odorico and Rigon*, 2003] ($k = 1, 2$ indicates surface and subsurface transport, respectively). Notice that by this assumption, preevent water is routed together with event water, thus accounting, albeit through a simplified approach [*Majone et al.*, 2004], for new water/old water dynamics [*McGuire et al.*, 2007; *Botter et al.*, 2008]. Also $f_{c_m}, f_{c_{m+1}}, \ldots, f_{c_n}(t)$ are the probability density functions of residence times in the channel reaches ($c_m \rightarrow c_{m+1} \rightarrow \ldots \rightarrow c_n$) linking hillslope h_γ to the outlet (the end section of reach c_n), which are assumed to have an inverse Gaussian form derived from the so-called parabolic model of the de Saint Venant equations [*Rinaldo and Rodriguez-Iturbe*, 1996]. In some of the following numerical experiments the parameters λ_k will be varied from their calibration values (see Table 1) in order to change the ratio between mean residence times in the hillslopes and in the channels.

Table 1. Calibration Parameters for the Hydrological Models of the Considered Catchments

Parameter[a]	Catchment						
	Brenta	Tanaro at Montecastello	Stura di Demonte	Orba at Casalcermelli	Bormida at Cassine	Tanaro at Alba	Tanaro at Farigliano
K^R_{sat}	22.7	25.9	25.9	25.9	25.9	25.9	25.9
θ_{FC}	0.22	0.15	0.15	0.15	0.15	0.15	0.15
ΔZ	285	1200	990	1050	300	390	300
η	0.8	0.72	0.22	0.96	0.64	0.40	0.8
a	3.5	0.9	2.4	3.0	1.2	1.8	1.5
D	1000	1000	1000	1000	1000	1000	1000
λ_1	1.5	0.6	2.1	2.8	0.9	3.0	1.2
λ_2	15	8.0	18.0	40	20	60	30

[a]Notation adopted for the parameters is as follows: K^R_{hsat} (mm h^{-1}) is the hydraulic conductivity at saturation for the reference soil; θ_{FC} is the soil water content at field capacity for the reference soil type; ΔZ (mm) represents the surficial soil thickness; η is the fraction of infiltrating water contributing to stream response; a (m s^{-1}) is the wave celerity ($a = (3/2)\,u$, where u is the uniform flow bankfull velocity); D (m^2 s^{-1}) is the hydrodynamic dispersion coefficient; λ_1 and λ_2 (h $(km^{-2})^{0.38}$) represent the parameters for the mean hillslope residence time for surface and subsurface flow, respectively.

[10] In the nonhomogeneous rainfall assumption, path probabilities are obtained, for each component, from the spatially distributed separation of rainfall into surface and subsurface contributions at each time t:

$$p_k(\gamma,t) = \frac{\int_{A\gamma} j_k(\mathbf{x},t)d\mathbf{x}}{\int_A j_k(\mathbf{x},t)d\mathbf{x}} = \frac{J_k(\gamma,t)}{J_k(t)};\ k = 1,2, \tag{3}$$

where A is the total catchment area, $\Sigma_{\gamma\in\Gamma}\, p_k\,(\gamma,t) \equiv 1\ \forall\ k$, t. In equation (3) $j_k(\mathbf{x},\ t)$ is the spatially distributed flux entering the system through the surface ($k = 1$) or the subsurface ($k = 2$) component at time t, $J_k(\gamma,t)$ is the total flux injected through path γ and component k, and $J_k(t)$ is the total flux injected through component k. Surface and subsurface flow rates at the basin outlet are then obtained by the time convolution of the corresponding fluxes with the appropriate (surface or subsurface) residence time distribution related with each possible path γ, weighted by the respective probability of occurrence:

$$Q_k(t) = \sum_{\gamma\in\Gamma} \int_0^t J_k(\gamma,\tau) f_\gamma(t-\tau)d\tau, \tag{4}$$

where path probabilities are explicitly accounted for by the net forcing $J_k(\gamma,t)$. Basin response to a rainfall event, once infiltration processes have been properly accounted for, is, thus, determined by the set of paths that are activated by the rainfall patterns and by the volume traveling through a given path relative to the total rainfall volume entering the basin. This is expressed in equation (4), where the pdf of the travel time distribution for a nonhomogeneous rainfall is expressed as the travel time pdf for a spatially uniform rainfall weighted through the probability that a given path γ be sampled by the nonuniform rainfall distribution.

[11] Rainfall spatial heterogeneity may, thus, exert an influence on the hydrologic response if distinct rainfall distributions produce significantly different samplings of the travel time distribution. A summary of the calibration of the models, with specific reference to the study catchments considered here, is given in section 3. Calibration and validation results are reported in Appendix A, while full details on the procedures are available in the literature [see, e.g., *Rinaldo et al.*, 2002; *Settin et al.*, 2005] as these are clearly outside the scope of this paper. Suffice here to note that the lumped character of the dynamics provided by the geomorphic approach, allowing, nonetheless, a fully distributed description of the geometry and topology of the basin, largely simplifies the noteworthy problems induced by validation procedures [e.g., *Beven and Binley*, 1992].

[12] In order to study the similarity among different probability distributions of travel times, or the lack thereof, we adopt a divergence measure, i.e., a measure of the distance between two or more probability distributions [*Wolpert and Macready*, 2007; D. H. Wolpert, Metrics for more than two points at once, 2004, available at http://arxiv.org/abs/nlin/0404032v1]. Several divergence measures are available, particularly in the information theory literature. Here we use the generalized Jensen-Shannon divergence (JSD), which has the advantage of providing a measure of the similarity among multiple probability distributions, rather than just of distribution pairs [*Lin*, 1991]. Given n probability distributions $\mathbf{p}_i = [p_i(1), p_i(2), \ldots, p_i(k)]$ ($i = 1, \ldots, n$; $j = 1, \ldots, k$ $\Sigma_{j=1}^k\, p_i(j) = 1$, $\forall i$; $0 \le p_i(j) \le 1\ \forall$ i, j), the generalized Jensen-Shannon divergence may be defined as [*Grosse et al.*, 2002]

$$\mathrm{JSD}(\mathbf{p}_1,\mathbf{p}_2,\ldots,\mathbf{p}_n) = H\left[\frac{1}{n}\sum_{i=1}^n \mathbf{p}_i\right] - \frac{1}{n}\sum_{i=1}^n H[\mathbf{p}_i], \tag{5}$$

where $H[\mathbf{p}] = -\Sigma_{j=1}^k\, p(j)\, \log_2 p(j)$ represents the Shannon entropy of $\mathbf{p}$ [*Shannon*, 1948]. The first term on the right-hand side of equation (5) represents the Shannon entropy of the average distribution, and the second one is the average entropy of the n distributions. It may be shown that the JSD is a positive definite measure [*Lamberti and Majtey*, 2003]:

$$\mathrm{JSD}(\mathbf{p}_1,\mathbf{p}_2,\ldots,\mathbf{p}_n) \ge 0, \tag{6}$$

where the equality holds if and only if $\mathbf{p}_1 = \mathbf{p}_2 = \ldots = \mathbf{p}_n$. The JSD is also invariant under any permutation of its arguments.

[13] A simplified version of runoff routing mechanisms has also been used in order to more directly explore the relative role of hillslope and channel processes. It simply consists in constructing the instantaneous unit hydrograph by assuming constant characteristic velocities for the hillslope (v_h) and channel states (v_h) [*Robinson et al.*, 1995;

Table 2. Characteristics of the Storm Events Considered for the Upscaling Experiments[a]

Catchment	Storm	Rain Gauge Density (Number of Gauges km^{-2})	I (km)	σ^2 (mm^2)
Brenta	7–17 July 1992	0.011	12.5	2.13
	25 September to 2 October 1992	0.012	16.5	1.45
	10–18 October 1996	0.009	25.0	1.18
	7–10 October 1998	0.005	20.0	1.31
	10–15 October 2000	0.012	18.5	1.65
Tanaro	2–12 November 1994	0.005	49.1	2.09
	12–20 October 2000	0.010	54.3	1.67
	14–19 July 2002	0.012	36.8	1.62
	14–30 November 2002	0.012	51.4	1.42
	21 November to 7 December 2003	0.005	41.5	1.81

[a]For each storm the reported variogram parameters were derived from hourly point observations by time-averaging the variogram estimates obtained for each time step and by a least squares fit with and exponential law (integral correlation scale I and spatial variance σ^2).

Botter and Rinaldo, 2003; *D'Odorico and Rigon*, 2003; *Saco and Kumar*, 2004], respectively, and neglecting runoff partitioning (thus, routing to the outlet the whole rainfall volume). In this formulation we consider all individual paths from each "pixel" site (i.e., 20 m $\times$ 20 m pixels in the digital elevation model) as determined from usual path and channel extraction procedures [e.g., *Tarboton*, 1997; *Rodriguez-Iturbe and Rinaldo*, 1997]. In brief, channelized portions of the catchment have been identified via a slope-dependent area threshold relying on proper determination of total contributing area through multiple flow direction algorithms in topographically convex areas. Flow pathways are determined by steepest descent directions. The choice of threshold, which commands considerable geomorphic effects, has been made by matching observed drainage density computed by analyzing whole distributions of unchanneled lengths for each subcatchment rather than the usual, rather insensitive Hortonian measure of total channelized length divided by area. Details are reported elsewhere [*Rinaldo et al.*, 2002; *Settin et al.*, 2005].

[14] The travel time distribution for the catchment is then determined by computing the travel time for each single path considering the assumed hillslope and channel celerities. This travel time distribution defines an instantaneous unit hydrograph which can be convoluted with space-time rainfall to determine the corresponding catchment response.

[15] The numerical experiments performed and discussed in section 4 are as follows. We generate 100 randomly located unit volume rainfall disks of radius R, and for each of them we determine the associated hydrologic response. We then compute the JSD(R) among all the hydrographs (which satisfy the requirements for the computation of the JSD, as the rainfall volume, and, thus, the area under the hydrographs are normalized) and repeat the procedure for 0.2 km $< R <$ 40 km. The number of disks considered (100) was determined through experiments to make sure that available transport paths were exhaustively sampled, particularly for small values of R. In fact, the shape of the JSD as a function of R was insensitive to further increments in the number of disks beyond about 100. In section 4 we describe the results of these analyses applied (1) to the full geomorphic model of the Brenta river catchment and (2) to the simplified transport model described above. The aim of numerical experiments performed was to relate the change in computed discharge directly to the characteristics of the forcing fields (i.e., in the eomorphic formulation, mean hillslope travel times are spatially variable at subcatchment scale, depending on subcatchment area).

3. Study Basins

[16] The analyses described in section 4 are based on the application of geomorphological models of the hydrologic response to the Brenta river basin (closed at Bassano del Grappa, Italy) and the Tanaro river basin (closed at Montecastello, Italy), developed for operational purposes [*Rinaldo et al.*, 2006a, 2006b]. The models have been tested on a large number of validation events (i.e., distinct from the events used for the calibration of their parameters). The robust reproduction of observed hydrographs under different hydrologic conditions indicates that the model indeed suitably describes the physical processes governing the

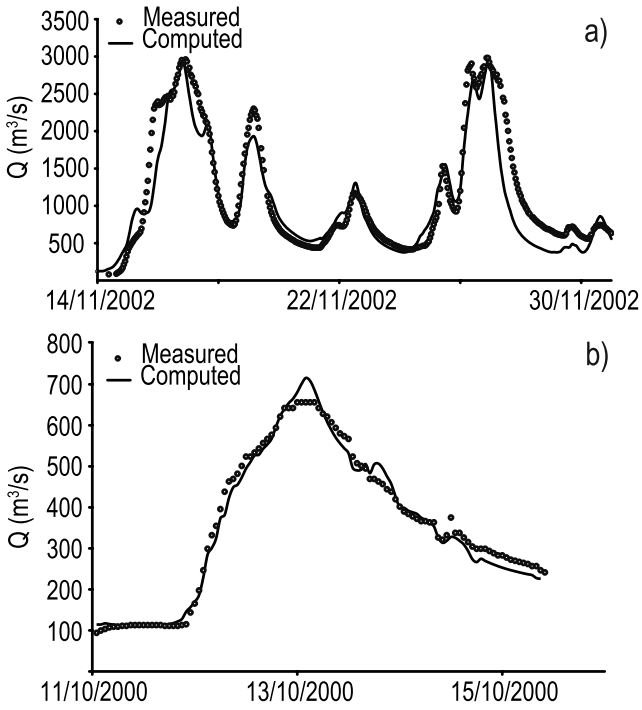

Figure 3. Samples of calibration and validation hydrographs for (a) the Tanaro river at Montecastello and (b) the Brenta river at Bassano del Grappa.

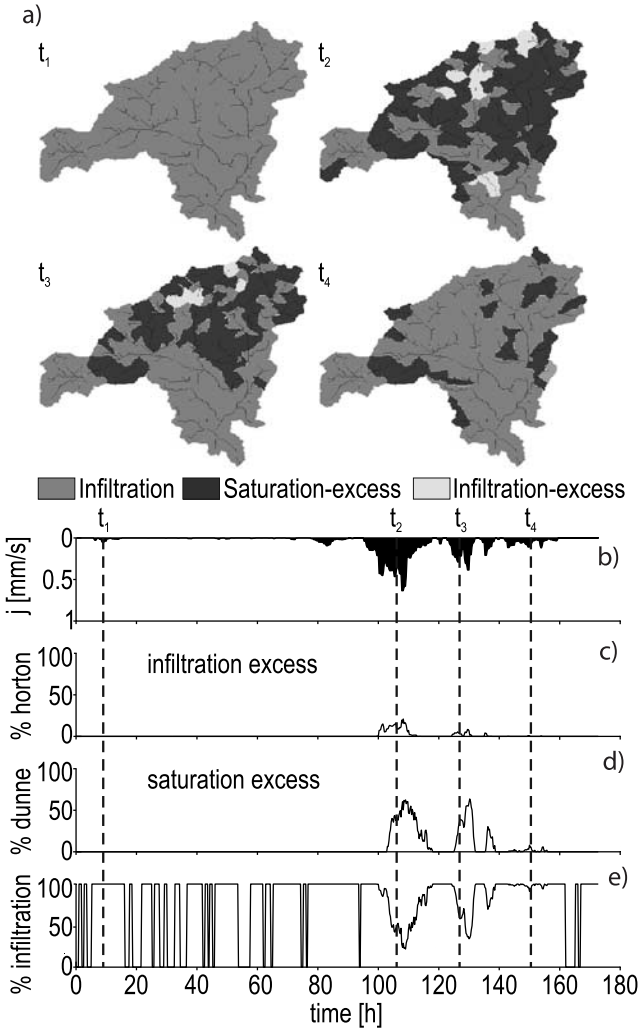

Figure 4. Infiltration and runoff generation mechanisms in the Brenta river. (a) The spatial distribution of areas where infiltration, saturation excess, and infiltration excess runoff are active is illustrated for sample time steps during a validation event (October 1993). In response to (b) the average rainfall over the catchment, (c) infiltration excess runoff provides only a modest contribution to the overall discharge (d) while saturation excess runoff occurs relatively more frequently. (e) Subsurface flow constitutes the largest contribution to the total discharge at the outlet.

hydrologic response. The two study basins were chosen to represent situations in which rainfall can be highly heterogeneous and to sample subbasins with a wide range of sizes (roughly $10-10^3$ km^2).

3.1. Tanaro River Catchment

[17] The Tanaro river is located in northwest Italy, in the alpine region south of Turin, Italy (Figure 1a). In the following, we consider several subbasins nested within the catchment closed at Montecastello, near the confluence with the Po river. The main stream length at Montecastello is about 276 km, and the area of the corresponding drainage basin is about 8000 km^2. The subbasins considered (see Figure 7) are Stura di Demonte at Gaiola (600 km^2), Tanaro at Farigliano (1500 km^2), Bormida at Carsine (1500 km^2), Orba at Casalcermelli (800 km^2), and Tanaro at Alba (3500 km^2).

[18] Soil type distribution is characterized using spatially distributed information from the local (Piemonte) Environmental Protection Agency. Differences are significant particularly between the alpine runoff-generating area (with values of saturated hydraulic conductivity in the range $K_{\mathrm{hsat}} \approx 10-30$ mm h^{-1}) and the downstream piedmont area ($K_{\mathrm{hsat}} \approx 0.3-1$ mm h^{-1}). Spatial differences in runoff-generating processes are accounted for by the Green-Ampt infiltration model as the governing parameters are defined for each hillslope on the basis of the spatially distributed information available.

[19] The rainfall regime in the Tanaro catchment is particularly heterogeneous both in space and time, with rainfall peaks located along the alpine foothills and minima located on the Alessandria plain. Rainfall data for the application of the hydrologic model were available via the rain gauge network operated by the Piemonte Environmental Protection Agency, with more than 100 gauging stations. Table 2 describes the information available for each storm event considered.

[20] The calibration of the hydrological model for the Tanaro river basin and its subbasins is based on observed hourly rainfall and discharge for the following five events: 12–20 October 2000, 14–19 July 2002, 14–30 November 2002, 21 November 2003 to 7 December 2003, and the catastrophic flood event of 2–12 November 1994. These calibration and validation events have also been used in the numerical experiments described in section 4.

[21] Sample calibration and validation curves are shown in Figure 3a, while a more complete account of the validation results is provided in Appendix A. Overall, the robust predictive capability of the model are established for different rainfall events, initial soil water content, etc. (for more details, see *Settin et al.* [2005]). We notice here that all calibration and validation events show a dominance of subsurface flow with respect to surface runoff (between 70% and 90% of total flow being due to subsurface transport), with some consequences for the interpretation of the subsequent analyses.

3.2. Brenta River Catchment

[22] The Brenta river is located in northeast Italy (Figure 1b). Its main alpine runoff-generating part, on which we focus here, has an area of 1560 km^2 and a main river course with length of about 72 km when closed at Bassano del Grappa. The rainfall patterns of the area are quite heterogeneous, with the heaviest rainfalls occurring mainly in the eastern part of the basin.

[23] Soil type and use in the Brenta river catchment are not uniform. In particular, a karstic area is present in the southwest portion of the basin, and spatial differences are accounted for through the local values of saturated hydraulic conductivity in the Green-Ampt infiltration model and of the fraction of infiltrated water lost to deep seepage.

[24] The numerical experiments performed on the Brenta river basin make use of observed hourly rainfall and discharge for the following five events: 7–17 July 1992, 25 September to 2 October 1992, 10–18 October 1996, 7–10 October 1998, and 10–15 October 2000. Such events have also been used in the numerical experiments described in section 4. Rainfall observations were acquired through a

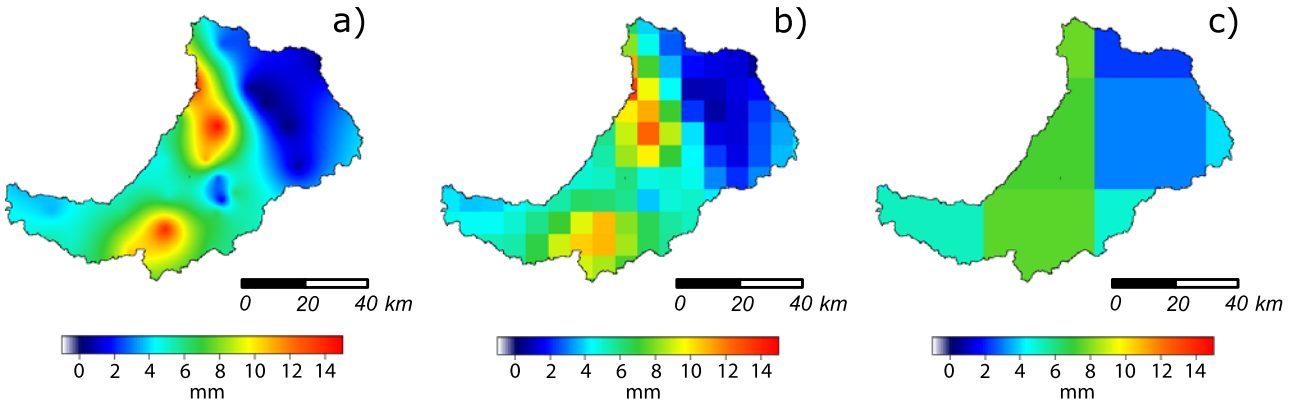

Figure 5. Representation of the rainfall upscaling procedure for the Tanaro river basin; spatial rainfall resolutions of (a) 0.1 km, (b) 10 km, and (c) 50 km.

network of 20 rain gauges operated by the Veneto and Trentino-Alto Adige Environmental Protection agencies. Table 2 provides a summary of the information available for each storm event considered.

[25] Sample calibration and validation curves are shown in Figure 3b. A more complete account of the validation results is provided in Appendix A. Also, in the case of the Brenta river the model proves robustly predictive for different rainfall events, initial soil water content, etc. (for more details, see *Uccelli et al.* [2004]). As for the Tanaro river, also, in the case of the Brenta river, total flow is dominated by subsurface runoff in all the events considered here (between 65% and 85% of the total flow volume is due to subsurface flow). Figure 4 illustrates, on one of the validation events, the dominant role of subsurface flow in the overall hydrologic response of the Brenta river, as most of the rainfall infiltrates into the soil (Figure 4d). When surface runoff occurs, this is mostly generated through the saturation excess mechanism rather than by infiltration excess (compare Figures 4b and 4c). The Tanaro river has a very similar behavior in this respect, as noted in section 3.1, and this circumstance will be important to the interpretation of some of the subsequent results.

4. Results and Discussion

4.1. Coarse Graining

[26] A set of coarse-graining (or upscaling) experiments has been performed to explore the effects of the spatial detail with which the rainfall forcing is prescribed on the response of the system. Thus, starting from the most refined grid resolution (0.1 km × 0.1 km) obtained by kriging rain gauge observations [*Zawadzki*, 1973; *Lebel et al.*, 1987], the hourly rainfall input fields of the calibration and validation storm events previously described are progressively coarse grained (Figure 5) up to a uniform distribution. In one set of experiments, rainfall values for each pixel with size $2\Delta x$ are obtained by averaging values in the four pixels of size Δx composing it (compare Figures 5b and 5c). This procedure does not strictly preserve the average rainfall volume entering the catchment at each time step because rainfall values pertaining to areas just outside the basin may enter the computation of the average rainfall for a coarse-grained pixel within the basin. This procedure is typically used when large-scale estima rainfall (say, from numerical weather forecasts) drive hydrological models. We will term this the "nonconservative" procedure throughout the rest of the paper. In order to isolate and analyze the effects of rainfall spatial detail alone a second, "conservative," procedure has been used, in which the computation of the average rainfall over a large-scale pixel crossing the catchment border is computed just over the small-scale pixels belonging to the catchment. Rainfall volume is, thus, exactly preserved.

[27] Experiments performed on the whole Brenta river basin indicate that differences in the hydrographs obtained

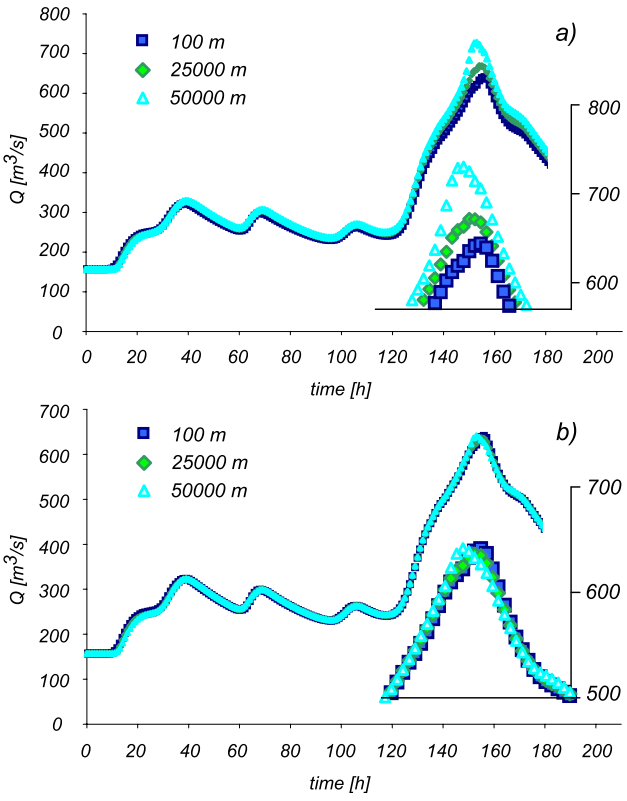

Figure 6. Flood hydrographs computed at Bassano del Grappa (Brenta river catchment) for the storm event of October 2000 for different rainfall aggregation scales. (a) Nonconservative and (b) conservative upscaling procedures.

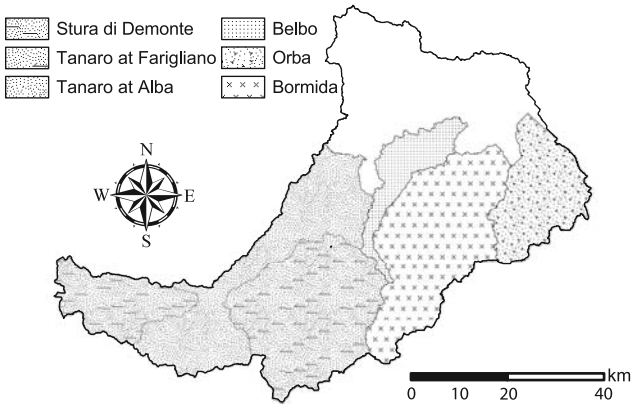

Figure 7. Subcatchments of the Tanaro river considered in the numerical experiments.

from rainfall fields with different resolutions emerge for the nonconservative upscaling procedure, particularly near the peak (Figure 6a, for the sample event of October 2000). On the contrary, differences are negligible in the conservative case (Figure 6b) even when a homogeneous rainfall is considered (for a pixel size larger than 50 km, a single pixel covers the entire basin). The comparison of the results from the conservative and nonconservative upscaling procedures is quite telling. It indicates that differences in the response of the system obtained from numerical experiments using the nonconservative procedure are simply the result of inaccurate representations of spatially averaged rainfall rather than of its spatial variability.

[28] The lack of significant differences in the conservative experiments is a partly unexpected result for a basin whose area ($O(10^3)$ km^2) is characterized by spatially variable properties. An interpretation can be provided by considering that the total flow volume at the outlet is dominated by subsurface flow. This is caused by (1) the local intensities, even in the high-resolution rainfall fields, not being large enough to trigger infiltration excess runoff and (2) the infiltrated volumes not being large enough to trigger significant saturation excess runoff (Figure 4). Upscaling rainfall fields reduces the local intensities but does not change the infiltrated volume, giving rise to a subsurface input which is very similar to that corresponding to high-resolution rainfall fields. Therefore, coarse graining of the rainfall fields does not appreciably change the separation of rainfall into surface and subsurface components. The lack of sensitivity to rainfall coarse graining furthermore requires transport mechanisms not be affected either, thus, requiring a more detailed investigation on how the selection of different transport paths changes by shifting rainfall patterns.

[29] We performed rainfall coarse-graining experiments on several subcatchments of the Tanaro basin (Figure 7). The results (Figure 8) confirm those obtained for the Brenta river. Provided the overall rainfall volume is preserved, rainfall variability in space does not play a major role for basins with areas ranging from 600 km^2 (Stura di Demonte at Gaiola) to 3500 km^2 (Tanaro at Alba). The spatial variability of rainfall becomes important only for the entire 8000 km^2 Tanaro catchment, where the model response exhibits a clear sensitivity to changes in rainfall resolution (see Figure 9a for a representative sample event). For aggregation scales up to 10 km, however, the model does not show appreciable changes in computed discharge as a response to the imposed rainfall resolution. It is worth noting that 0.1 km was chosen as the finest resolution for the spatial interpolation of rainfall fields to match the resolution of other spatially distributed information (i.e., digital terrain model, soil data, land use data). As reported in Table 2, this resolution is greater than the average distance among available rain gauges, which is appropriate from an

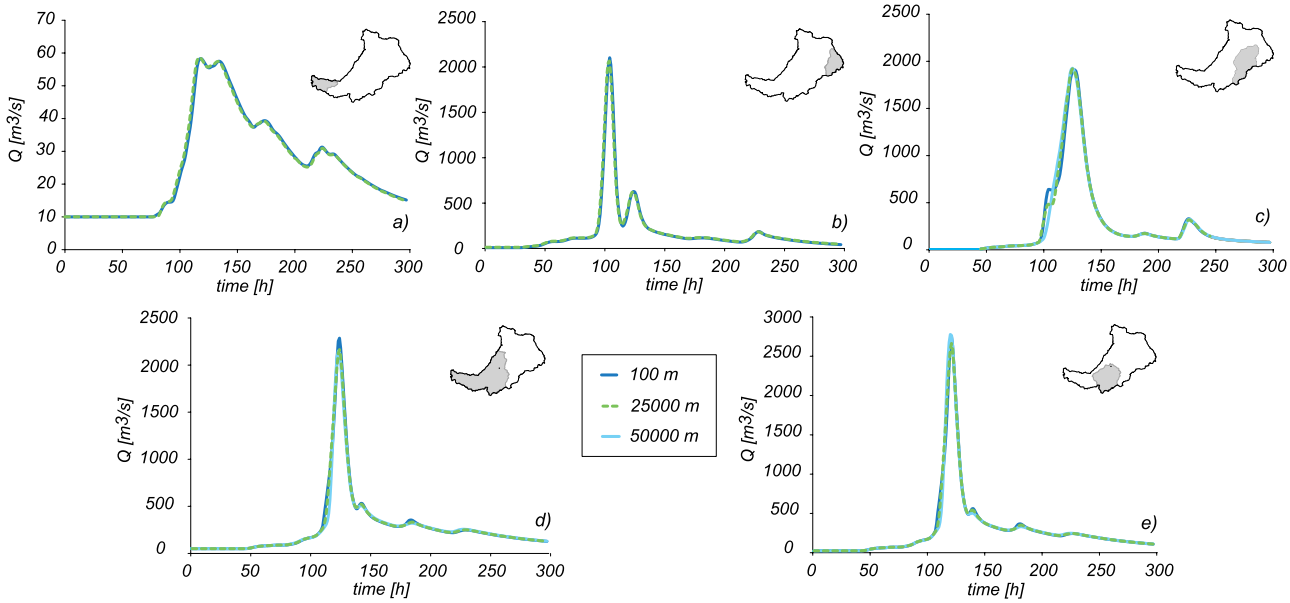

Figure 8. Simulated discharges for a sample of the investigated subcatchments of the Tanaro basin. Spatial resolutions of rainfall ranges from 100 m up to homogeneous rainfall over the considered subcatchment. (a) Stura di Demonte (600 km^2), (b) Orba (800 km^2), (c) Bormida (1500 km^2), and (d) Tanaro at Alb 0 km^2).

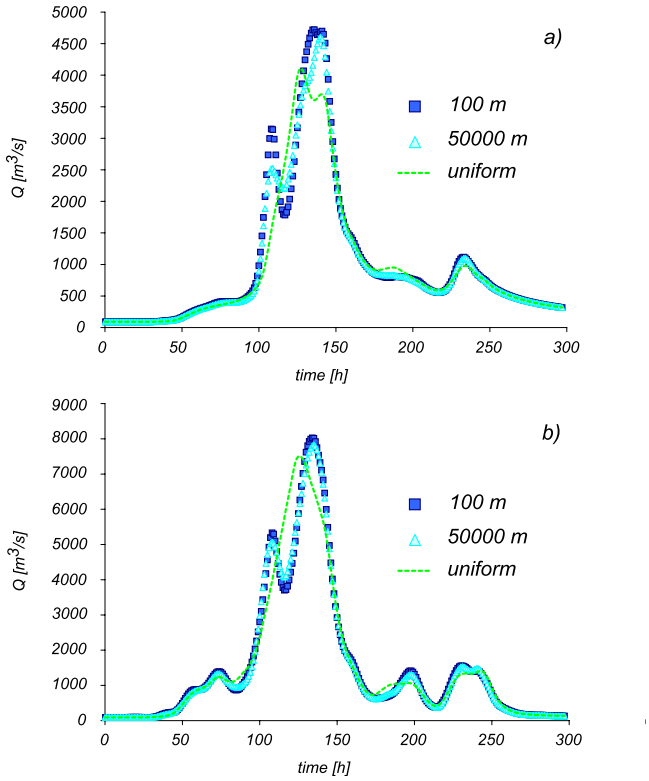

Figure 9. Computed discharge at Montecastello (Tanaro river catchment) for the storm event of November 1994 and for different rainfall aggregation scales (conservative procedure) (a) with and (b) without infiltration.

operational viewpoint because of the large rainfall correlation scales implied by the large-scale frontal nature of the storm events typical of the area.

[30] The insensitivity to the upscaling of rainfall is due to the dominance of subsurface flow pathways, as noted above for the Brenta river, which are not affected by changes in the resolution of the rainfall fields and to an unexpected relative invariance of residence time distributions sampled by different rainfall patterns. In order to clarify the relative roles of these two factors we next separate the effects of sampling transport paths and of spatial heterogeneities in runoff production processes by "switching off" the runoff generation model. We, thus, assume the soil to be everywhere completely impervious. The resulting flood hydrographs (Figure 9b) only exhibit moderate changes for rainfall aggregations up to 50 km and show that only a uniform rainfall (at resolution of 150 km) produces a significant difference in basin response. These results, compared to those from the model properly incorporating runoff separation processes, strongly suggest that the observed dependency of the hydrologic response on rainfall resolution can in this case be chiefly ascribed to heterogeneous soil characteristics rather than to the effects of the spatial variability (in Euclidean space) of transport paths along the drainage directions and of the associated travel and residence times.

[31] It is, of course, relevant to determine under what circumstances the interplay of rainfall and transport path heterogeneities does play a role in the determination of the hydrologic response. We, thus, perform numerical experiments in which the spatial heterogeneity of synthetic and simplified rainfall distributions is varied and then characterize the differences in the sampled travel time distributions and in the associated hydrologic responses.

4.2. Travel Time Distributions Sampled by Heterogeneous Rainfall

[32] As indicated in equation (4), the possible influence of rainfall heterogeneity may be exerted by a selective sampling of the population of available travel paths. This may be investigated by studying the travel time probability density functions as sampled by idealized rainfall distributions. Here we assume a unit volume rainfall of duration 1 h, which is uniform within a disk of radius R (and zero elsewhere). The aim of this experimental setup is to study how the travel time distributions sampled by one such rainfall disk, randomly placed in space, change at changing disk dimensions and transport processes within the basin.

[33] The response of the numerical model of the Brenta river basin, for three sample unit volume rainfall disks of radius R = 5 km (one such disk occupies approximately 5%

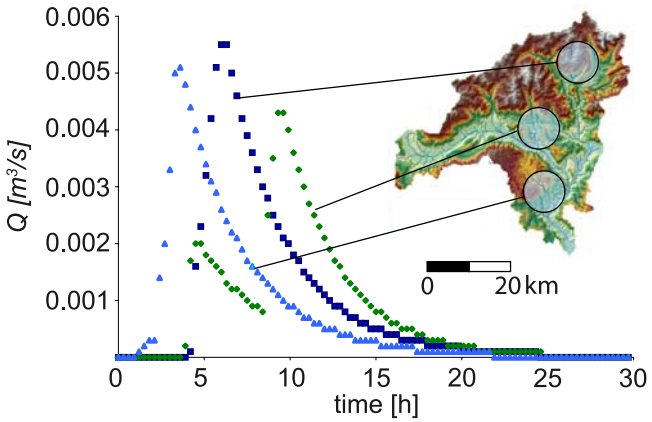

Figure 10. Hydrologic response of the Brenta river at Bassano del Grappa for three idealized rainfall patterns with unit volume and R = 5

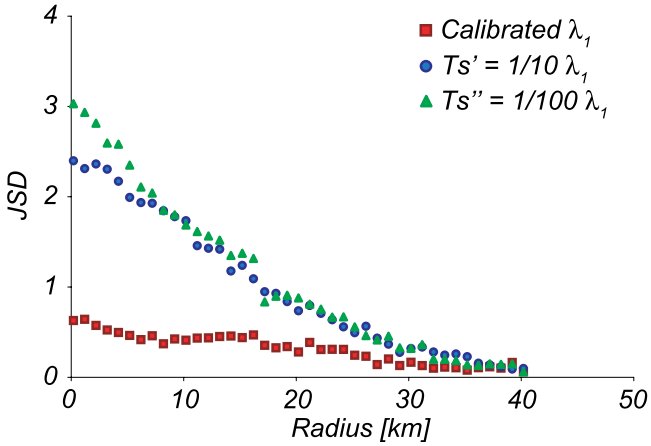

Figure 11. Jensen-Shannon divergence among the responses to 100 randomly placed unit volume rainfall disks versus disk radius for the Brenta catchment. High JSD values indicate a lack of similarity among the randomly sampled responses.

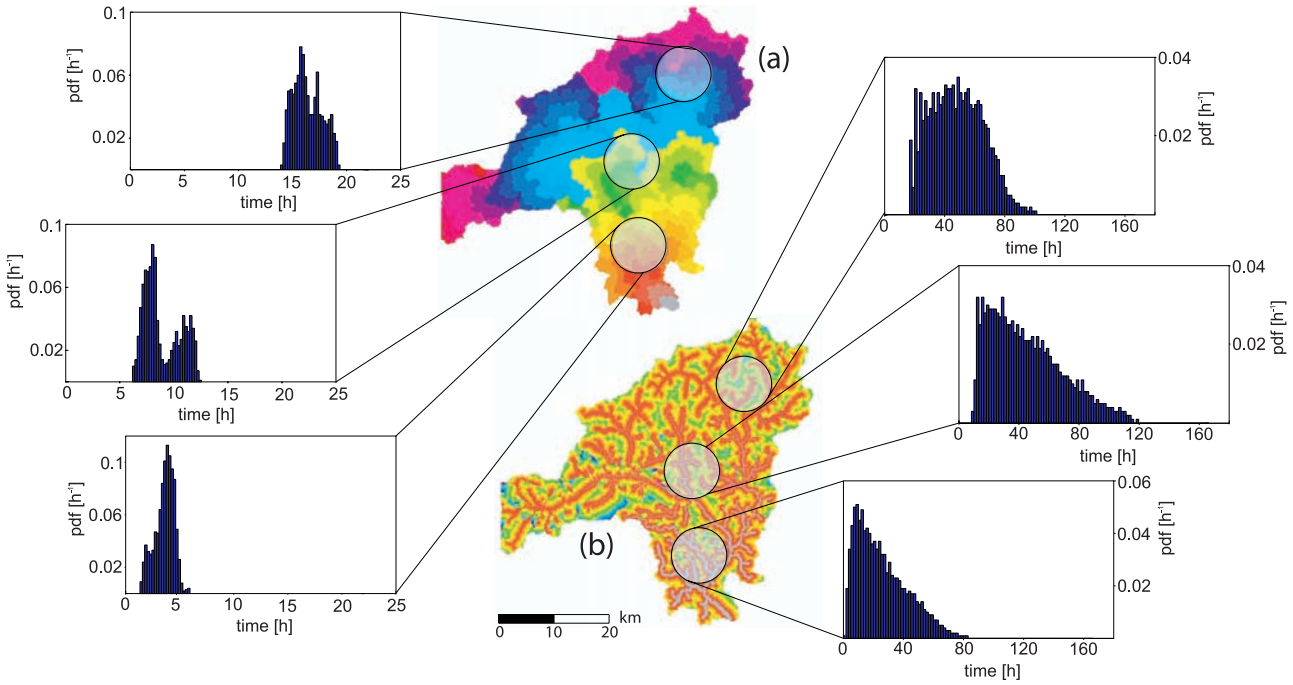

Figure 12. Sample travel time probability density functions obtained with the simplified, kinematic, transport model for two v_c/v_h ratios: (a) v_c/v_h = 1/1 and (b) v_c/v_h = 1/0.01.

of the whole Brenta catchment), highlights the similarities among the computed hydrographs, with a relatively minor effect of rainfall location (Figure 10). In this experiment the infiltration has been switched off in order to account only for runoff routing effects on the computed discharge. The JSD divergence among the hydrographs generated by different rainfall disks applied to the Brenta river basin (Figure 11) decreases rapidly with disk diameter. Interestingly, when mean hillslope travel times, $\bar{t}_{\gamma,1} = \lambda_1 \times A_\gamma^{0.38}$ [*Boyd*, 1978; *D'Odorico and Rigon*, 2003], are decreased (by decreasing the controlling parameter λ_1), the differences among catchment responses excited by different randomly placed disks are increased (Figure 11). This observation can be interpreted by noting that the time spent by water parcels within hillslopes typically dominates the total residence time within a catchment because the channelized part of a path is typically relatively short and is traversed with a much higher velocity [*Botter and Rinaldo*, 2003]. A decrease in the mean hillslope residence time, thus, tends to attenuate its dominance, and the results of Figure 11 point to the role of hillslope versus channel transports in determining the sensitivity of the catchment response to rainfall heterogeneity.

4.3. Role of Hillslope and Channel Processes

[34] As in the previous experiments with the full Brenta river model, we generate several (100) randomly located rainfall disks of radius R (varying from 0.4 to 100 km), and for each of them we determine the associated response at the outlet of the basin using the simplified kinematic transport model, which allows a clearer control of hillslope and channel residence times (e.g., see Figure 12). We then compute JSD(R) for different kinematic ratios, v_c/v_h, and for different basins in order to characterize the degree of similarity among the sampled probability density functions as a function of the characteristic size of rainfall events and of different ratios of hillslope/channel velocities (and, thus, different ratios of hillslope/channel residence times). The velocity values in channeled and unchanneled pixels clearly strongly affect the resulting travel time distributions (Figure 13), but the divergence among system responses as a function of R quickly and monotonically decreases as the ratio v_c/v_h is increased. In the following, we focus on two contrasting cases (Figure 13): (1) $v_c/v_h = 1\ \mathrm{m\ s^{-1}}/1\ \mathrm{m\ s^{-1}}$, in which hillslope and channel transport proceeds at the same rate, and (2) $v_c/v_h = 1\ \mathrm{m\ s^{-1}}/0.01\ \mathrm{m\ s^{-1}}$, which provides a more realistic representation of the relative importance of hillslope and channel residence time of actual catchments [*Botter and Rinaldo*, 2003]. In this latter case the travel time distribution is largely dominated by the larger and heterogeneous travel time within hillslope states. As expected,

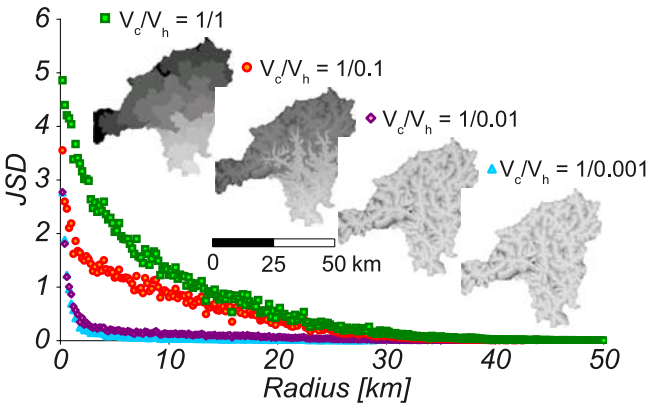

Figure 13. JSD(R) plots for different v_c/v_h ratios in the Brenta river catchment. Lower velocity ratios produce larger differences in the hydrologic response at the catchment outlet.

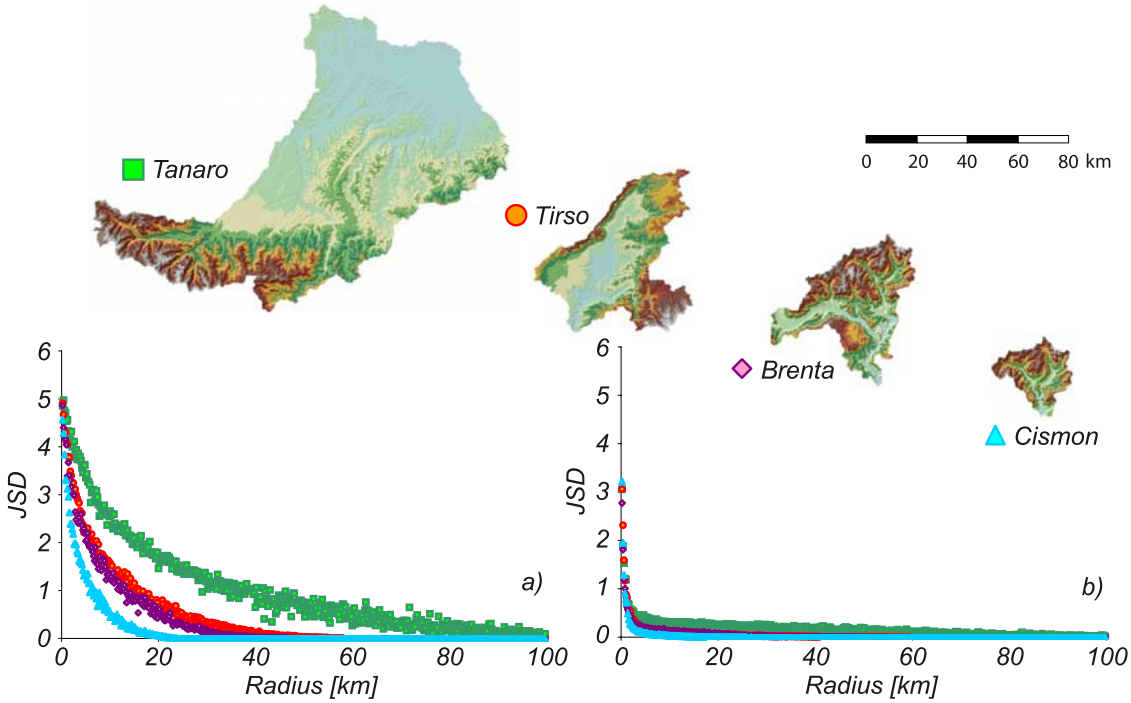

Figure 14. Sample JSD(R) plots for four study catchments with different sizes in the range 800 km^2–8000 km^2 and to two velocity ratios: (a) v_c/v_h = 1/1 and (b) v_c/v_h = 1/0.01.

differences among travel time distributions selected by disk rainfall again decrease when the disk diameter is increased (Figure 14) because larger disks sample a larger amount of the available paths. Differences in travel time probability density functions are greater when the velocities of water parcels in the hillslope and in the channels are equal (i.e., v_c/v_h = 1, Figure 14a). In this case, differences in travel times among different paths can be quite substantial. On the contrary, when the velocity is realistically much smaller in the hillslopes than in the channels (i.e., v_c/v_h = 100, Figure 14b), the differences among travel time distributions are drastically reduced even for small rainfall disks (i.e., small scales of rainfall heterogeneity). In this case, travel times are dominated by the time spent in the hillslope, and, thus, as long as the rainfall heterogeneity scale is larger than the typical hillslope size (less than 1–2 km^2), any rainfall distribution will sample all the possible heterogeneous paths and, thus, produce approximately the same response. Finally, it is worth noting that the sensitivity of the response of the system to different rainfall disks is noticeably larger in larger catchments when v_c/v_h = 1 (JSD values for the Tanaro basin are shown in green in Figure 14a, while those for Cismon are shown in blue). On the other hand, differences in sensitivity are greatly reduced in the more realistic case v_c/v_h = 100 (JSD curves are very close to one another in Figure 14b).

5. Conclusions

[35] Geomorphological models of the hydrologic response greatly simplify Monte Carlo-like analyses of the type pursued herein for their greater computational ease yet maintaining a fully unabridged description of the catchment and also for certain issues on validation, especially non-uniqueness of parameter estimates, owing to the lumped description of the dynamics. The analyses performed for several subbasins in the Brenta and Tanaro river systems with areas up to 8000 km^2 indicate that as may be expected, flood responses are most sensitive to the average rainfall instantaneously injected into the catchment (Figures 6 and 8). It follows that even in the case of quite large basins (with area indicatively up to several thousand square kilometers), the key role of dense rain gauge networks lies in their ability to estimate the total volume of precipitation falling over the region rather than in the characterization of the spatial variability of a storm. Our results suggest that when saturation excess runoff-generating mechanisms are dominant, the critical element that insures insensitivity of hydrologic response to spatial variability of precipitation is the proper estimation of the total rainfall volume over the catchment in time. As noted in section 4, this is because the spatial scales of variability of rainfall are very often much larger than the typical hillslope scale. Whenever infiltration excess mechanisms are important, the spatial distribution of areas of intense rainfall may be an important factor in determining the hydrologic response, and an interesting open issue is the study of the interplay between the scales of heterogeneity of rainfall and of soil type and use. A further relevant issue on which investigation is needed relates to proper tools for estimating the instantaneous rainfall volume over a catchment given point measurements in the presence, say, of orographic effects inducing nonstationary rainfall fields.

[36] The spatial distribution of rainfall does play an important role in the case of large catchments (as in the case of the Tanaro river, with area of about 8000 km^2, Figure 9a) because the transport paths sampled by rainfall are in this case very heterogeneous because of the impor-

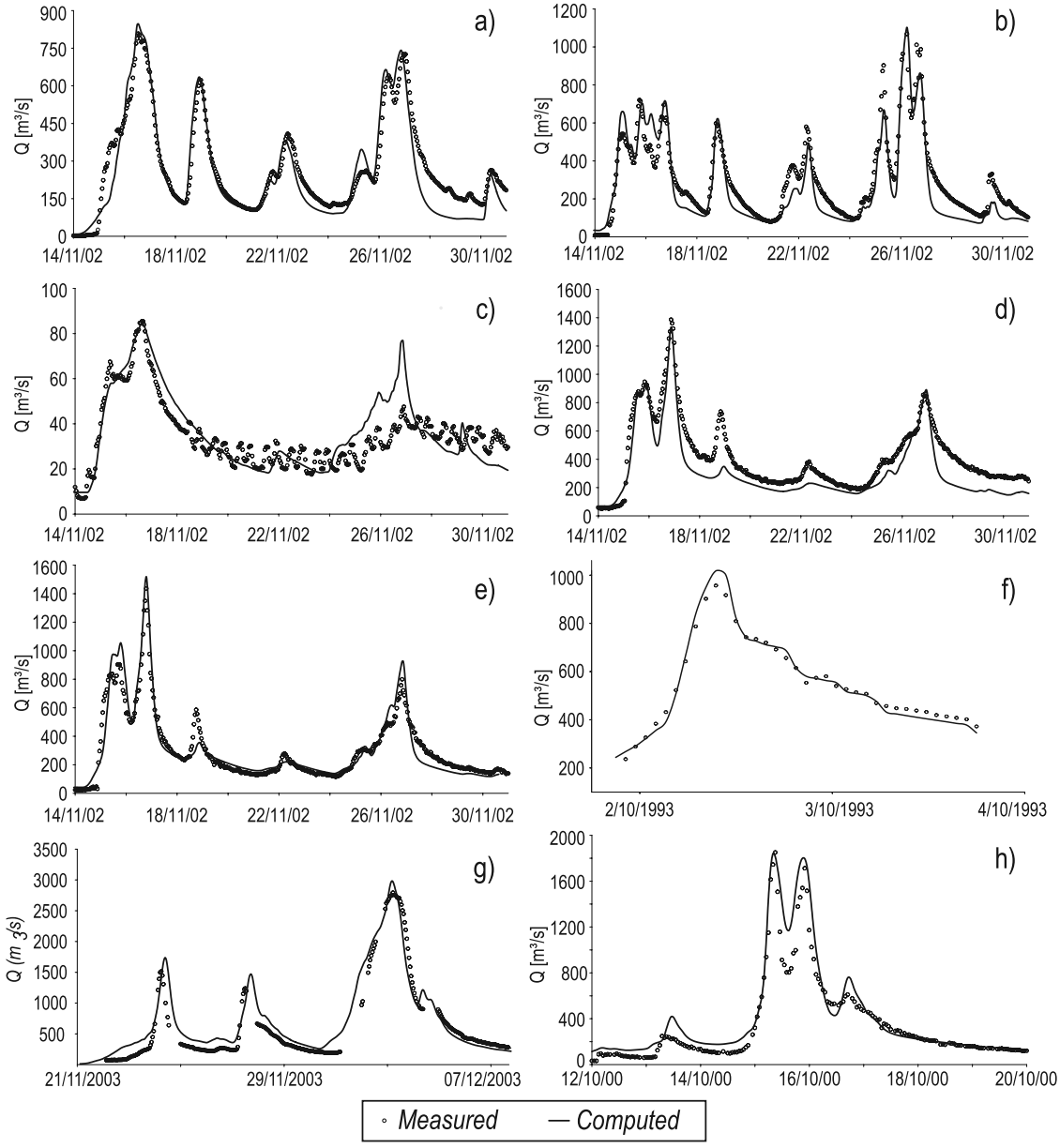

Figure A1. Computed versus measured discharge for the subcatchments of Tanaro system (calibration event of November 2002): (a) Bormida at Cassine, (b) Orba at Casalcermelli, (c) Stura di Demonte at Gaiola, (d) Tanaro at Alba, and (e) Tanaro at Farigliano. In the other plots sample validation events for (f) Brenta, (g) Tanaro closed at Montecastello, and (h) Tanaro closed at Farigliano are shown.

tance of channel residence times. Nonlinear infiltration and saturation excess runoff-generating mechanisms induce a moderate sensitivity to rainfall spatial distribution in the cases considered here (e.g., see differences in the peak discharge in Figure 9a) because the total discharge at the outlet is dominated by subsurface flow. The sensitivity of flood response to rainfall heterogeneity is likely to be important in hydrological systems where infiltration excess is the dominant runoff-generating mechanism because local rainfall intensity decreases as a result of rainfall aggregation at coarser spatial scales.

[37] "Switching off" infiltration processes in the model and, therefore, forcing all variability to arise because of water transport processes showed that even at the 8000 km^2 scale, rainfall variability induces only a moderate variability in the flood response (Figure 9b). Analyses using idealized rainfall distributions suggest a physically based interpretation of these observations, linked to the properties of the travel time distributions sampled by rainfall patterns. Because the total travel time of a water parcel within a catchment is dominated by its travel time within the hillslope, the hillslope size controls the sensitivity of the hydrologic response to rainfall distributions. As long as the characteristic spatial correlation scale of rainfall is larger than the typical hillslope scale the sampled travel time distributions are quite independent of the specific instanta-

neous rainfall patterns, which, therefore, do not exert an appreciable influence on the resulting flood response even for catchment areas of several thousand square kilometers. This inference may be confirmed by, e.g., considering the length of each channel reach between two subsequent confluences as representing the linear size of the associated hillslope. The overall hillslope characteristic size may be computed as the average of all such lengths. The hillslope characteristic size defined in this manner for our nine study basins ranges from 2.25 to 2.72 km, in very good agreement with the value of R for which an abrupt change in the slope of JSD(R) occurs (see Figures 13 and 14b). As anticipated, for rainfall pattern sizes beyond this threshold value the specific rainfall distribution does not play an appreciable role in determining the hydrologic response of the system (the value of JSD(R) remains very small, indicating a very high similarity among all sampled hydrographs). In the case of real rainfall patterns the size of the idealized rainfall distributions used here may be substituted by a characteristic size, e.g., defined as the integral scale of the autocorrelation function of rainfall fields. Because values of the integral scale commonly encountered in frontal systems are typically larger than 10 km [also see *Zawadzki*, 1973; *Lebel et al.*, 1987; *Bacchi and Kottegoda*, 1995] while characteristic hillslope sizes are usually less than a few kilometers, our results indicate that in this case, the spatial distribution of rainfall does not play a significant role in the generation of the catchment response. For large catchments (or, arguably, for peculiarly shaped ones, e.g., displaying a marked elongation) the residence time in the channel may be expected to increase significantly and to be closer to the hillslope travel time (similar to the $v_c = v_h$ case, see Figure 14a). The spatial distribution of rainfall becomes a main controlling factor in this case.

[38] Our results seem to clarify the relative role of hillslope versus channel travel time distributions in determining the sensitivity of the hydrologic response to rainfall spatial variability. We believe that these findings suggest a reconciliation of previous contrasting results and provide theoretical and practical guidance to develop general and robust hydrological models.

Appendix A: Performances of the Hydrological Models

[39] The performance of the hydrological models adopted for the numerical experiments described has been tested for different storm events for all the catchments to which the complete geomorphologic model has been applied. This appendix summarizes model performances by portraying (1) full calibration results obtained for the five subcatchments of Tanaro system (see Figure 7) examined in our analyses (Figures A1a–A1e) and (2) samples of computed versus measured discharge for different validation events, also used for the previous analyses, and different catchments (Figures A1f–A1h).

[40] **Acknowledgments.** The authors wish to thank three anonymous reviewers for the discussions and insight provided. Funding from the EU research project AQUATERRA (GOCE 505428) and the PRIN 2006 National research project Fenomeni di trasporto idrologici: Formulazioni lagrangiane, ruolo di eterogeneitá, effetti morfologici, processi stocastici a scala di bacino is gratefully acknowledged. Support from the research projects RIMOF2 (Fondazion di Risparmio di Verona, Vicenza, Belluno and Ancona) and MODITE (Cariverona) is also gratefully acknowledged.

References

Bacchi, B., and N. T. Kottegoda (1995), Identification and calibration of spatial correlation patterns of rainfall, *J. Hydrol.*, *165*, 311–348.

Barry, D., J.-Y. Parlange, L. Li, D.-S. Jeng, and M. Crapper (2005), Green-Ampt approximations, *Adv. Water Resour.*, *28*, 1003–1009, doi:10.1016/j.advwatres.2005.03.010.

Beven, K., and A. Binley (1992), The future of distributed models: Model calibration and uncertainty prediction, *Hydrol. Processes*, *6*, 279–298.

Botter, G., and A. Rinaldo (2003), Scale effect on geomorphologic and kinematic dispersion, *Water Resour. Res.*, *39*(10), 1286, doi:10.1029/2003WR002154.

Botter, G., F. Peratoner, M. Putti, A. Zuliani, R. Zonta, A. Rinaldo, and M. Marani (2008), Observation and modeling of catchment-scale solute transport in the hydrologic response: A tracer study, *Water Resour. Res.*, *44*, W05409, doi:10.1029/2007WR006611.

Boyd, M. J. (1978), A storage-routing model relating drainage basin hydrology and geomorphology, *Water Resour. Res.*, *14*(5), 921–928.

Brath, A., and A. Montanari (2003), Sensitivity of the peak flows to the spatial variability of the soil infiltration capacity for different climatic scenarios, *Phys. Chem. Earth*, *28*, 247–254.

Chu, S. T. (1978), Infiltration during an unsteady rain, *Water Resour. Res.*, *14*(3), 461–466.

Dingman, S. L. (Ed.) (1994), *Physical Hydrology*, 575 pp., Macmillian, New York.

D'Odorico, P., and R. Rigon (2003), Hillslope and channel contributions to the hydrologic response, *Water Resour. Res.*, *39*(5), 1113, doi:10.1029/2002WR001708.

Dodov, B., and E. Foufoula-Georgiou (2005), Incorporating the spatio-temporal distribution of rainfall and basin geomorphology into nonlinear analyses of streamflow dynamics, *Adv. Water. Resour.*, *28*, 711–728, doi:10.1016/j.advwatres.2004.12.013.

Eagleson, P. S. (1978), Climate, soil, and vegetation: 1. Introduction to water balance dynamics, *Water Resour. Res.*, *14*(5), 705–712.

Gabellani, I., G. Boni, L. Ferraris, J. von Hardenberg, and A. Provenzale (2007), Propagation of uncertainty from rainfall to runoff: A case study with a stochastic rainfall generator, *Adv. Water Resour.*, *30*, 2061–2071, doi:10.1016/j.advwatres.2006.11.015.

Goovaerts, P. (Ed.) (1997), *Geostatistics for Natural Resources Evaluation*, 483 pp., Oxford Univ. Press, New York.

Green, W., and G. Ampt (1911), Studies on soil physics, 1: The flow of air and water through soils, *J. Agric. Sci.*, *4*(1), 1–24.

Grosse, I., P. Bernaola-Galván, P. Carpena, R. Román-Roldán, J. Oliver, and H. Stanley (2002), Analysis of symbolic sequences using the Jensen-Shannon divergence, *Phys. Rev. E*, *65*(4), 041905, 1–16, doi:10.1103/PhysRevE.65.041905.

Krajewski, W. F., V. Lakshmi, K. P. Georgakakos, and C. J. Subashi (1991), A Monte Carlo study of rainfall sampling effect on a distributed catchment model, *Water Resour. Res.*, *27*(1), 119–128.

Lamberti, P., and A. Majtey (2003), Non-logarithmic Jensen-Shannon divergence, *Physica A*, *329*, 81–90, doi:10.1016/S0378-4371(03)00566-1.

Lashermes, B., and E. Foufoula-Georgiou (2007), Area and width functions of river networks: New results on multifractal properties, *Water Resour. Res.*, *43*, W09405, doi:10.1029/2006WR005329.

Lebel, T., G. Bastin, C. Obled, and J. Creutin (1987), On the accuracy of areal rainfall estimation: A case study, *Water Resour. Res.*, *23*(11), 2123–2134.

Lin, J. (1991), Divergence measures based on the Shannon entropy, *IEEE Trans. Inf. Theory*, *37*(1), 145–151.

Lovejoy, S., and D. Schertzer (1985), Generalized scale invariance in the atmosphere and fractal models of rain, *Water Resour. Res.*, *21*(8), 1233–1250.

Majone, B., A. Bellin, and A. Borsato (2004), Runoff generation in karst catchments: Multifractal analysis, *J. Hydrol.*, *294*, 176–195.

Marani, M. (2005), Non-power-law scale properties of rainfall in space and time, *Water Resour. Res.*, *41*, W08413, doi:10.1029/2004WR003822.

Marani, M., G. Grossi, F. Napolitano, M. Wallace, and D. Entekhabi (1997), Forcing, intermittency, and land surface hydrologic partitioning, *Water Resour. Res.*, *33*(1), 167–175.

McGuire, K. J., M. Weiler, and J. J. McDonnell (2007), Integrating tracer experimentes with modeling to assess runoff processes and water tranist times, *Adv. Water Resour.*, *30*, 824–837.

Rinaldo, A., and I. Rodriguez-Iturbe (1996), The geomorphological theory of the hydrologic response, *Hydrol. Processes*, *10*(6), 803–829.

Rinaldo, A., A. Bellin, M. Ferri, M. Marani, R. Rigon, A. Fornasiero, and S. Silvestri (2002), Modellazione matematica del bacino del Fiume Brenta (chiuso a Bassano del Grappa), *Tech. Rep. 09-02*, Univ. of Padua, Padua, Italy.

Rinaldo, A., G. Botter, E. Bertuzzo, A. Uccelli, T. Settin, and M. Marani (2006a), Transport at basin-scales: 1. Theoretical framework, *Hydrol. Earth Syst. Sci.*, *10*, 19–26.

Rinaldo, A., G. Botter, E. Bertuzzo, A. Uccelli, T. Settin, and M. Marani (2006b), Transport at basin-scales: 2. Applications, *Hydrol. Earth Syst. Sci.*, *10*, 31–48.

Robinson, J. S., M. Sivapalan, and J. D. Snell (1995), On the relative roles of hillslope processes, channel routing, and network geomorphology in the hydrologic response of natural catchments, *Water Resour. Res.*, *31*(12), 3089–3101.

Rodriguez-Iturbe, I., and A. Rinaldo (Eds.) (1997), *Fractal River Basins: Chance and Self-Organization*, 564 pp., Cambridge Univ. Press, New York.

Rodriguez-Iturbe, I., M. Marani, P. D'Odorico, and A. Rinaldo (1998), On space-time scaling of cumulated rainfall fields, *Water Resour. Res.*, *34*(12), 3461–3469.

Saco, P. M., and P. Kumar (2004), Kinematic dispersion effects of hillslope velocities, *Water Resour. Res.*, *40*, W01301, doi:10.1029/2003WR002024.

Salvucci, G., and D. Entekhabi (1995), Hillslope and climatic controls on hydrologic fluxes, *Water Resour. Res.*, *31*(7), 1725–1739.

Segond, M., H. Wheater, and C. Onof (2007), The significance of spatial rainfall representation for flood runoff estimation: A numerical evaluation based on the Lee catchment, UK, *J. Hydrol.*, *347*, 116–131, doi:10.1016/j.jhydrol.2007.09.040.

Settin, T., et al. (2005), Modello matematico della risposta idrologica del Fiume Tanaro (chiuso ad Alessandria), *Tech. Rep. 11-05*, Univ. of Padua, Padua, Italy.

Shah, S., P. O'Connell, and J. Hosking (1996), Modelling the effects of spatial variability in rainfall on catchment response. 2. Experiments with distributed and lumped models, *J. Hydrol.*, *175*, 89–111.

Shannon, C. (1948), A mathematical theory of communication, *Bell Syst. Tech. J.*, *27*(379–423), 623–656.

Smith, J. A., M. L. Baeck, K. L. Meierdiercks, P. A. Nelson, A. J. Miller, and E. J. Holland (2005), Field studies of the storm event hydrologic response in an urbanizing watershed, *Water Resour. Res.*, *41*, W10413, doi:10.1029/2004WR003712.

Tarboton, D. (1997), A new method for the determination of flow directions and upslope areas in grid digital elevation models, *Water Resour. Res.*, *33*(2), 309–320.

Uccelli, A., T. Settin, M. Marani, and A. Rinaldo (2004), Sui modelli matematici di fondamento geomorfologico: Telerilevamento e produzione di deflusso, paper presented at the XXIX Convegno di Idraulica e Costruzioni Idrauliche, Gruppo Ital. di Idraulica, Trento, Italy.

Wilson, C. B., J. B. Valdes, and I. Rodriguez-Iturbe (1979), On the influence of the spatial distribution of rainfall on storm runoff, *Water Resour. Res.*, *15*(2), 321–328.

Winchell, M., H. V. Gupta, and S. Sorooshian (1998), On the simulation of infiltration- and saturation-excess runoff using radar-based rainfall estimates: Effects of algorithm uncertainty and pixel aggregation, *Water Resour. Res.*, *34*(10), 2655–2670.

Wolpert, D. H., and W. G. Macready (2007), Using self-dissimilarity to quantify complexity, *Complexity*, *12*(3), 77–85.

Zawadzki, I. I. (1973), Statistical properties of precipitation patterns, *J. Appl. Meteorol.*, *12*, 459–472.

E. Alessi Celegon, M. Marani, L. Nicótina, and A. Rinaldo, Dipartimento di Ingegneria Idraulica, Marittima, Ambientale e Geotecnica, Universitá di Padova, Via Loredan 20, I-35131 Padova, Italy. (marani@idra.unipd.it)